Langmuir−Blodgett Mono- and Multilayers of (Di)alkoxy-Substituted Poly(*p*-phenylenevinylene) Precursor Polymers. 1. Langmuir Monolayers of Homo- and Copolymers of (Di)alkoxy-Substituted Precursor PPVs

J. G. Hagting, R. E. T. P. de Vos, K. Sinkovics, E. J. Vorenkamp, and A. J. Schouten*

Department of Polymer Science, University of Groningen, Nijenborgh 4, 9747 AG Groningen, The Netherlands

Received January 20, 1999; Revised Manuscript Received March 25, 1999

ABSTRACT: The Langmuir monolayer behavior of (di)alkoxy-substituted precursor poly(*p*-phenylenevinylenes) (PPVs) with a methoxy-leaving group was studied. The average orientation of the aromatic ring and the ether groups at the air−water interface was elucidated by external FT-infrared reflection spectroscopy measurements at the air−water interface combined with FT-IR computer simulations. The aromatic rings of the precursors, except those of the dibutoxy-substituted one, take on, directly after spreading, an almost perpendicular orientation to the water subphase. The isotherms of these precursors showed no special transitions, and these polymers can be considered to be in a condensed or 2-D collapsed state with lateral cohesive $\pi-\pi$ interactions between the aromatic rings as the most prominent interaction leading to this condensed state. The aromatic rings of the dibutoxy-substituted precursor are lying flat at the water surface at large areas per repeating unit and can be considered to be in the expanded state directly after spreading. The isotherm of this precursor showed two transitions because here the chain conformation is predominantly determined by the butyl chains and not by the main chain.

Introduction

The Langmuir−Blodgett (LB) technique makes it possible to organize molecules into highly ordered monolayers and produce multilayers with desired architectures.[1,2] However, these architectures often suffer from poor mechanical and thermal properties.[3−5] Due to stronger intra- and intermolecular interactions, polymeric LB films tend to have better thermal and mechanical stability than low molecular weight compounds.[6−8] For many of today's and future applications in, for instance, micro- and optoelectronics, ultrathin polymer films are needed.[9,10] However, the techniques available for preparing these films are limited. Spin-coating and self-assembly techniques are often applied,[11,12] but both suffer from their own disadvantages. Spin-coating does not give good films when molecular weights are low or the general film forming properties of the polymer are insufficient. Moreover, thicknesses down to one molecular layer are not possible, and the spin-coating technique leads in principle to randomly oriented polymer chains and monomeric units. Self-assembly has the disadvantage that the polymer chain has to be chemically modified, and this might be detrimental to build in functionality or to moisture sensitivity in the case of using strong ionic or polar groups.

The Langmuir−Blodgett technique with polymers as spreading materials can in principle cope with these problems and even has additional advantages such as orientation of the functional groups at the backbone, flow-induced orientation during transfer, resulting in oriented polymers in transferred monolayers, and in almost unlimited possibilities for complex architectural design. Suitable polymeric spreading materials, however, also have to meet certain requirements, and unexpected phenomena might show up during the study of and attempts to prepare these complex layers.

Certain polymers appeared to be suitable spreading materials for the LB technique.[13] Looking at the backbone type, one can distinguish flexible and stiff (rigid rod) polymers. Examples of both types have been studied and, depending on the substituents, found to be suitable LB materials, although both classes behave quite differently in the monolayer state and during the transfer step. Some examples of flexible LB polymers are poly(dimethylsiloxane),[14] poly(vinyl alcohol),[15] poly(octadecyl methacrylate),[16] poly(vinyl stearate),[17] stereoregular poly(methyl methacrylate)s,[17] and poly(vinyl acetate-*co*-vinyl stearates)s.[18] Examples of suitable rigid rod polymers include polyglutamates,[19,20] substituted polysaccharides,[21] and polyisocyanides.[22]

It is well-known that isotherms of low molecular compounds can be divided more or less analogous to the 3-D state in a gaseous phase, a liquid (condensed) state, and several condensed states. Analogously to 3-D polymeric states, one can also find 2-D "dissolved", condensed, and crystalline states.[23] Moreover, during transfer of rigid rod polymers or 2-D crystals, flow-induced orientation can take place, leading to the unique possibility of 2-D oriented polymeric films. In that case polymers are able to attain such a random 2-D conformation with a maximum of contacts with water that a very thin polymeric monolayer is obtained. Depending on the balance between lateral cohesive interactions and adhesive interactions (hydration forces) with the water, polymers can take on a 2D "collapsed" coil conformation or a 2-D "dissolved" state. This leads to completely different states of these monolayers. The first one is called the condensed state, comparable to a precipitated glassy polymer or concentrated phase separated case. The second one is called the expanded state, which can be compared to a polymer in solution.

Poly(*p*-phenylenevinylene)s (PPVs) are main chain conjugated polymers which have interesting electrical and photoconducting properties, making them suitable

10.1021/ma9900683 CCC: $18.00
Published on Web 05/15/1999

Scheme 1

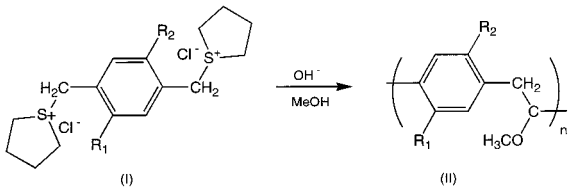

(I) (II)

Precursor polymer (II)	R1	R2
prec-MePPV	H	OCH_3
prec-DMePPV	OCH_3	OCH_3
prec-DBuPPV	OC_4H_9	OC_4H_9
prec-BuMePPV	OCH_3	OC_4H_9
copolymer	OCH_3 or OC_4H_9	OCH_3 or OC_4H_9
prec-MEHPPV	OCH_3	$OCH_2CH(CH_2CH_3)C_4H_9$

to be applied in optoelectronic and microelectronic devices.[24] The use of the LB technique can be very useful in obtaining desired structures of these conjugated polymers.[25] PPVs are rigid rod polymers which are insoluble, unless they are substituted with long alkyl chains.[26] Therefore, nonsubstituted or short alkyl chain substituted PPVs cannot be used for the LB technique. However, PPVs can be prepared by thermal treatment of water-soluble precursor polyelectrolytes with a sulfonium-leaving group or by a chloroform-soluble precursor with a methoxy-leaving group.[27,28] The water-soluble precursor can be made suitable for use in the LB technique by replacing the chlorine counterion with a soaplike counterion[29,30] or by a bilayer-forming amphiphile.[31] It is also possible to use the chloroform-soluble precursor polymer with a methoxy-leaving group.[32]

In part 1 of this paper we studied the monolayer behavior of dialkoxy-substituted precursor PPVs with a methoxy-leaving group. We used alkoxy-substituted precursors to obtain a good interaction of the polymer with the water phase. The monolayer behavior upon compression of the precursors was studied by surface pressure and by hysteresis experiments. External reflection IR spectra of the precursor PPVs at the air−water interface were measured. Spectral simulations were done to determine the orientation of the repeating units of the polymer at the air−water interface. An energy minimization program was used to determine the conformation of the ether groups in the monolayer.

The stability, transfer, and multilayer structure of alkoxy-substituted precursor PPVs will be described in part 2.

Experimental Section

Materials. The syntheses of the monomers (disulfonium salts (**I**)) have been described by others.[33,34] The sulfonation reaction to synthesize the monomer of precursor poly(2-methoxy-5(2′-ethyl)hexoxy-1,4-phenylenevinylene) (prec-MEHPPV) was done with 30 equiv of tetrahydrothiophene instead of the normally used 3 equiv. The synthesis route of the precursor polymers (**II**) is shown in Scheme 1. These polymerization reactions, except for the synthesis of precursor (2-methoxy-1,4-phenylenevinylene) (prec-MePPV), were done by adding an ice-cold N_2-purged solution of 0.3 M sodium hydroxide in methanol to an ice-cold purged solution of 0.3 M sulfonium salt in methanol. After 1 h of reaction under N_2 and mechanical stirring, the solution was allowed to reach room temperature, and a precipitate was formed. The precipitate was rinsed with methanol, dissolved in chloroform, and precipitated in ice-cold ether or methanol and dried. The polymerization reaction of prec-MePPV was done in water instead of methanol. The reaction was quenched after 20 min. The solution was neutralized (pH = 7) with a HCl solution (1 M). The neutralized solution was dialyzed against water (1 day) and methanol (3 days). Subsequently, the dialyzed solution was heated to 50 °C under a N_2 flow, and a precipitate was formed. The precipitate was rinsed with methanol, dissolved in chloroform, and precipitated in ice-cold ether.

The precursor copolymer was synthesized by mixing the monomers in a molar ratio of 1:1. From ^{1}H NMR a molar ratio in the copolymer of 1:1 was determined. The yields of the polymerization reactions were about 40%.

GPC. Gel permeation chromatography (GPC) measurements were performed on 2 mg/mL solutions in a Spectra Physics AS 1000 system using universal calibration with a Viscotek H-502 viscometer and a Shodex RI-71 refractive index detector. $CHCl_3$ was used as eluent. The columns were calibrated with polystyrene standards.

LB. The surface pressure isotherms and the stabilization experiments were carried out on a computer-controlled Lauda Filmbalance (FW 2). The surface pressure could be measured with an accuracy of 0.05 mN/m. The subphase was water, purified by reverse osmosis and subsequent filtration trough a Milli-Q purification system. The polymers were spread from chloroform solutions (Uvasol quality, concentrations 0.2−0.4 mg/mL). The solutions were stored in the dark, and a drop of pyridine was added to prevent premature elimination by acidic products in chloroform.[34] Pressure−area diagrams were measured at various speeds (1−10 Å^2/(repeating unit min)) and various temperatures (5−40 °C). Hysteresis experiments were carried out with compression speeds of 1 Å^2/(repeating unit min) with a pause of 5 min and were carried out on the Lauda-Filmbalance (FW 2).

IR. External reflection spectroscopy of the monolayers at the air−water interface was performed using a Specac monolayer/grazing angle accessory (P/N 19650 series) in a Mattson Galaxy 6021 FT-IR spectrometer. The light was polarized by a BaF_2 wire-grid polarizer. When p-polarized light is used, the electric field will have two components, one parallel and one perpendicular to the interface, but the first one will dominate the spectrum.[35] When s-polarized light is used, the electric field only has a component parallel to the interface. Consequently, the information obtained from both polarization directions will be similar. However, the amount of energy reaching the detector is lower for p-polarization than for s-polarization, and therefore, we used s-polarization. A reflection angle of 30° was used because at this angle the noise level is relatively low and the absorptions relatively high.[35] The spectra were recorded with a resolution of 8 cm^{-1}, and 4000 scans were taken. An external reflection spectrum of the clean water surface was used as a reference for the spectra. Unfortunately, it was not possible to simultaneously perform surface-pressure measurements. Therefore, the amount of precursor polymer applied (chloroform solution, Uvasol quality, concentration 0.04−0.05 mg/mL) and the surface area of the trough in the monolayer accessory were determined as exact as possible. After spreading the necessary amount of polymer solution and the evaporation of the solvent, the area of the monolayer

was reduced to 25%. The monolayers were allowed to relax at least 15 min before the spectra were collected.

Spectra Simulations. The IR-reflection spectrum of a thin film at the air−water interface is different from the transmission spectrum of the film due to optical and dispersion effects. Consequently, knowledge of the differences in the spectra caused by these effects is crucial for the interpretation of the spectroscopic data and must be done before relating any differences in the band shape, position, and intensity to structural, orientational, and/or chemical bonding changes in the film. Therefore, spectrum simulations have been used to elucidate the influence of these optical effects and to make comparison of the various spectra possible.[35−37]

The optical constants of the polymers, necessary for the spectrum simulations, were calculated according to the following procedure. A transmission spectrum of a free-standing film of the polymer was used as an input spectrum. The thickness of this film and the refractive index were estimated on the basis of the amplitude of the interference fringes and their periodic spacing. The absorption coefficients were converted into wave vector (k) values after which the refractive index (n) spectrum could be calculated from the estimated k-spectrum with the Kramers−Kroning relationship.[36] For prec-DMePPV and prec-DBuPPV the real part of the refractive index was centered at 1.55 and 1.5, respectively. For the optical constants of water wavenumber-dependent n and k values from the *Infrared Handbook* were used.[38]

Energy Minimizations. The minimizations of the energy of the molecule were done based on an MM2 force field in CS CHEM3D which includes a new implementation of Norman L. Allinger's MM2 force field.[39]

Results and Discussion

Surface-Pressure Isotherms. The average molecular weights of all the polymers determined by gel permeation chromatography (GPC) experiments are rather high ($\bar{M}_w \approx 1 \times 10^6$ and $M_n \approx 3 \times 10^5$). Therefore, experiments were carried out to check that a real monolayer was formed, in which all polymer segments are in contact with the water surface. Crisp emphasized that a true polymer monolayer is formed when the polymer sample occupies a maximum and reproducible area upon spreading with different solvents or spreading solution concentrations.[40] We found, for all the precursor polymers used, that the area was reproducible when the concentration of the spreading solutions was varied (0.04−0.9 mg/mL). Precursor poly(2,5-dibutoxy-1,4-phenylenevinylene) (prec-DBuPPV), prec-MEHPPV, and precursor poly(2-methoxy-5-butoxy-1,4-phenylenevinylene) (prec-BuMePPV) can be dissolved in chloroform and in toluene, and changing the solvent had no influence on the isotherms either. So, although these polymers have rather high molecular weights, it appears that, after spreading, all segments are in contact with water, no crossovers are formed, and a true polymer monolayer is obtained.

During compression of high molecular weight polymer monolayers, surface-pressure gradients might be built up.[41] If surface-pressure gradients are present in the monolayer, the isotherm obtained should be dependent on the compression speed and the film size. We studied the influence of the compression speed and the film size on the isotherms and found that the isotherms almost coincide. So, it can be concluded that no large surface-pressure gradients are present in these monolayers.

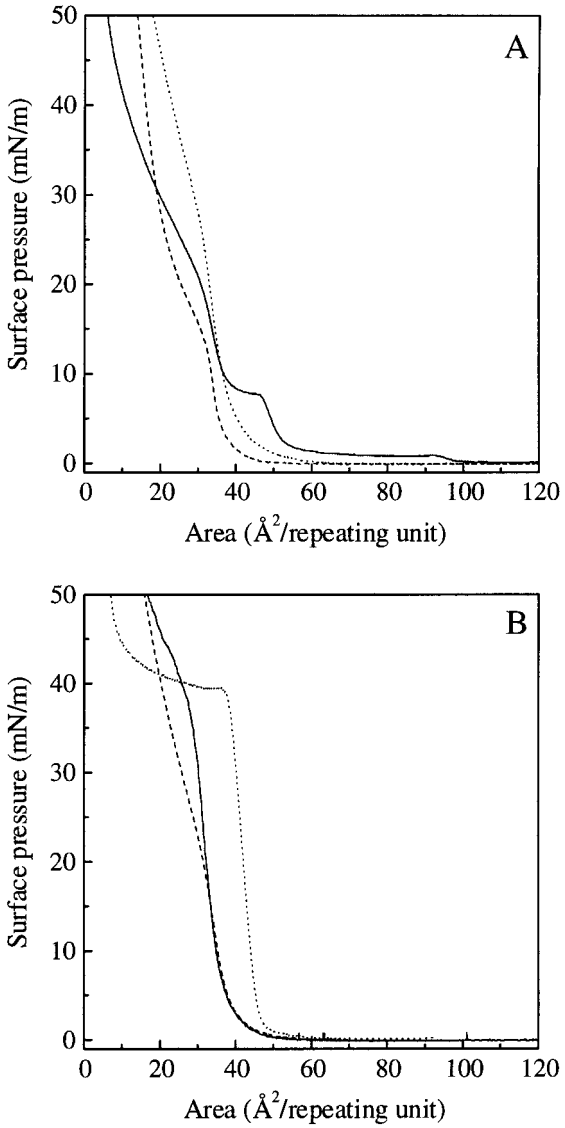

Figure 1. Pressure−area isotherms of (A) prec-DMePPV (dotted line), prec-MePPV (dashed line), and prec-DBuPPV (solid line) and (B) prec-BuMePPV (solid line), copolymer (dashed line), and prec-MEHPPV (dotted line). T = 20 °C, compression speed 5 Å²/(repeating unit min).

Figure 1A shows the surface-pressure isotherms of precursor poly(2,5-dimethoxy-1,4-phenylenevinylene) (prec-DMePPV), prec-MePPV, and prec-DBuPPV. The isotherms of prec-DMePPV and prec-MePPV (Figure 1A, dotted curve and dashed curve, respectively) do not exhibit any special transitions and can be explained considering the polymer in a 2-D "collapsed" state (this state should not be confused with the 3-D collapsed film), resulting in a monolayer consisting of separate coils that cohere due to lateral forces. These cohesive lateral forces are thus responsible for the 2-D collapsed coils and for the aggregation of these coils in larger domains as well. The absence of any measurable surface pressure at larger areas is in agreement with such a condensed state. Upon compression, these domains (islands) are pushed together and slowly deform until a close-packed monolayer film of prec-DMePPV and prec-MePPV is obtained at a surface area of 38 and 36 Å²/repeating unit, respectively. These values do not agree with a completely flat orientation of the molecules, because, as deduced from CPK models, the rise in the surface pressure for prec-DMePPV and prec-MePPV

should be expected at about 68 ± 2 and 57 ± 2 Å^2/repeating unit, respectively.

Should the aromatic rings be oriented perpendicular to the surface, the area per repeating unit would be independent of the substituents and about 34 ± 2 Å^2/repeating unit. Therefore, the values obtained correspond with a state where the aromatic rings of the repeating units of prec-DMePPV and prec-MePPV are oriented more or less perpendicularly to the surface.

The isotherm of prec-DBuPPV (Figure 1A, solid curve) shows two transitions: the first at about 100 Å^2/repeating unit and the second at about 48 Å^2/repeating unit. The first transition might be easy to explain, taking into account that from CPK models an area of 100 ± 5 Å^2/repeating unit could be calculated for a "flat" orientation. This means that at areas larger than 100 Å^2/repeating unit the aromatic rings and the butyl chains are lying completely flat on the water surface. When the two butyl substituents are oriented more or less perpendicular to the surface and the aromatic ring of prec-DBuPPV is lying completely flat on the water surface, the calculated area is about 68 Å^2/repeating unit. This area does not correspond with the area of 48 Å^2/repeating unit, so the second transition does not agree to this situation. Because prec-DMePPV and prec-MePPV do not show such transitions, it is very likely that the conformation of prec-DBuPPV in the monolayer is determined by the butyl chains.

The isotherms of other butyl-substituted precursor polymers—the copolymer (see Scheme 1) and prec-BuMePPV—can be seen in Figure 1B. Although prec-BuMePPV (Figure 1B, solid curve) and the copolymer (Figure 1B, dashed curve) are also substituted with butyl chains, no transitions are seen in the isotherms. Similar to prec-DMePPV, both polymers show the closely packed monolayer state at about 38 Å^2/repeating unit. Presumably, in the prec-BuMePPV and in the copolymer case, the conformation and the orientation of the polymer in the monolayer are more or less analogous to prec-DMePPV with dominating cohesive lateral forces between the backbone elements. Apparently, the butyl side chains only dominate the conformation and the orientation of the polymer when the butyl chains are in a closely packed state as in prec-DBuPPV.

The isotherm of prec-MEHPPV (Figure 1B, dotted curve), a precursor substituted with a branched alkyl chain, also does not show any transitions. In this case, the closely packed monolayer state in this case is found at an area of 45 Å^2/repeating unit, which is larger than the area of the closely packed monolayer states found for prec-DMePPV and prec-BuMePPV. From CPK models it was deduced that if the repeating unit of prec-MEHPPV is lying completely flat with respect to the water surface, the area would be about 105 Å^2/repeating unit, and if only the aromatic ring is lying flat and the alkyl chain is oriented out of the water surface, the area would be about 68 Å^2/repeating unit. Therefore, we assume that the rings are standing perpendicular to the water surface with the alkyl chain oriented out of the water subphase, thus forming an amphiphilic monolayer. The alkyl chains of this amphiphilic monolayer are branched and therefore do not crystallize but are in the "liquid state". For alkyl chains in the liquid state at the interface a minimum of free energy is obtained at a certain interchain distance due to attractive long-range London/van der Waals forces and repulsive short-range forces.[42] It is assumed that this minimum of free energy is obtained at an area of 45 Å^2/repeating unit and that repulsive forces between the branched side chains prevent the backbone elements to pack as closely as in the case of prec-DMePPV and prec-BuMePPV.

The influence of temperature on the isotherms of prec-DMePPV, prec-DBuPPV, and prec-MEHPPV is shown in Figure 2.

The isotherm of prec-DMePPV (Figure 2A) and prec-DBuPPV (Figure 2B) is shifted to a larger area per repeating unit at lower temperatures. The same influence of the temperature on the isotherm was found for prec-MePPV and prec-BuMePPV. From stabilization experiments it was found that this is not a kinetic effect. Monolayers of poly(ethylene oxide) (PEO) exhibit a similar temperature dependence.[43] It is known that upon decreasing temperature the solvent quality of water with respect to the PEO segments improves, leading to stronger hydration forces. We assume that in the case of these precursors the hydration forces of the ether groups also increase with decreasing temperature, leading to a less condensed monolayer with a larger area per repeating unit. Moreover, the transitions in the isotherm of prec-DBuPPV more or less fade away at higher temperatures (Figure 2B), resulting in an isotherm that resembles more the isotherm of prec-DMePPV. Apparently, at higher temperatures the conformation is less determined by the butyl chains.

In the case of prec-MEHPPV the collapse pressure decreases with increasing temperature as can be seen in Figure 2C. However, a temperature-dependent shift in the isotherm as was described above for the other precursors is not found. The backbone elements of prec-MEHPPV are already less closely packed due to the branched alkyl chain, and it is assumed that therefore no temperature-dependent shift is found.

Summarizing, only the prec-DBuPPV case transitions in the isotherm are found. To investigate these transitions further, FT-IR reflection measurements at the air−water interface and hysteresis experiments were carried out.

FT-IR Reflection Spectroscopy at the Air−Water Interface. Figure 3 shows the results of the FT-IR reflection spectroscopy experiment of prec-DMePPV monolayer at the air−water interface. The experimental spectra were taken at about 80, 52, 35, and 25 Å^2/repeating unit. These positions in the isotherm are shown in the inset of Figure 3; the corresponding spectra are parts a, b, c (solid line), and d, respectively. The assignments and the transition moment directions of the absorptions of prec-DMePPV are given in Table 1. The FT-IR reflection spectroscopy was carried out with s-polarization. Therefore, only vibration modes with a component in the plane of the interface will absorb.[23] This means that when the intensity of an absorption band is weak compared to the calculated spectrum, the dipole transition moment of this band is on average oriented perpendicularly to the air−water interface.

When the measured spectra of Figure 3a−c are compared, it can be seen that the absorbances increase upon compression but that the mutual ratios of the bands do not change significantly. This means that the conformation and the orientation of the units in the polymer are the same at all these areas per repeating unit and do not change during compression.

To study the orientation of the closely packed monolayer with an area of 35 Å^2 per repeating unit (Figure

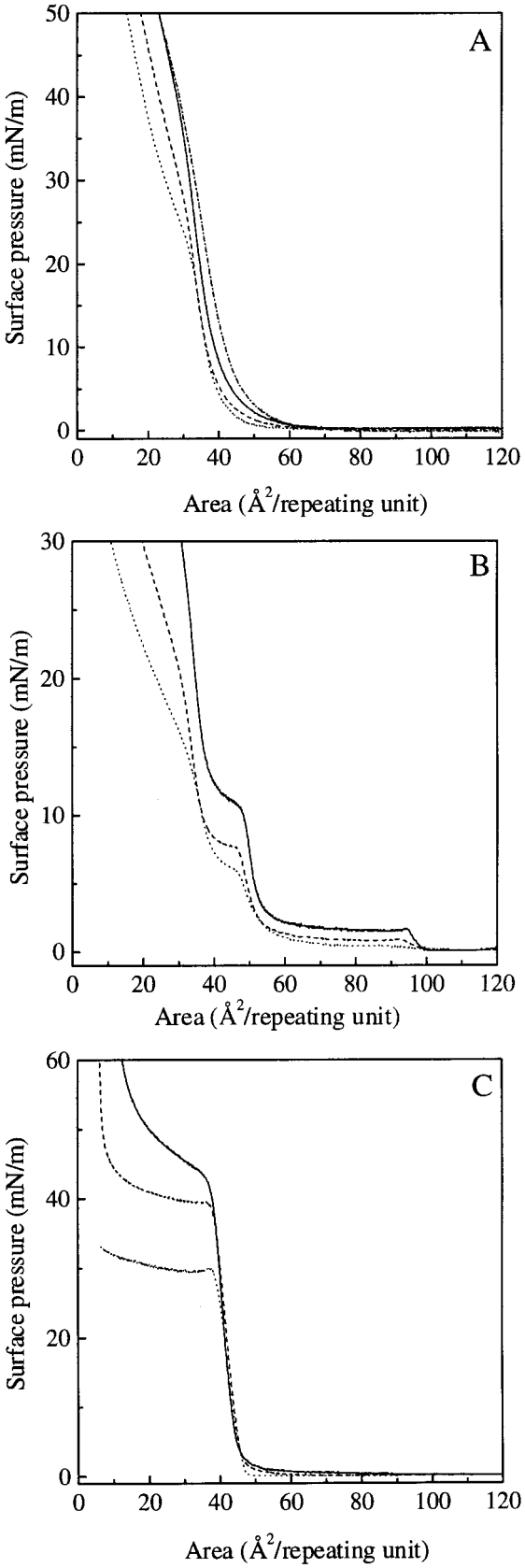

Figure 2. Influence of temperature on the pressure−area isotherms of (A) prec-DMePPV, (B) prec-DBuPPV, and (C) prec-MEHPPV. Temperature: 6 °C (dash−dotted line), 10 °C (solid line), 21 °C (dashed line), and 38 °C (dotted line). Compression speed: 5 Å²/(repeating unit min).

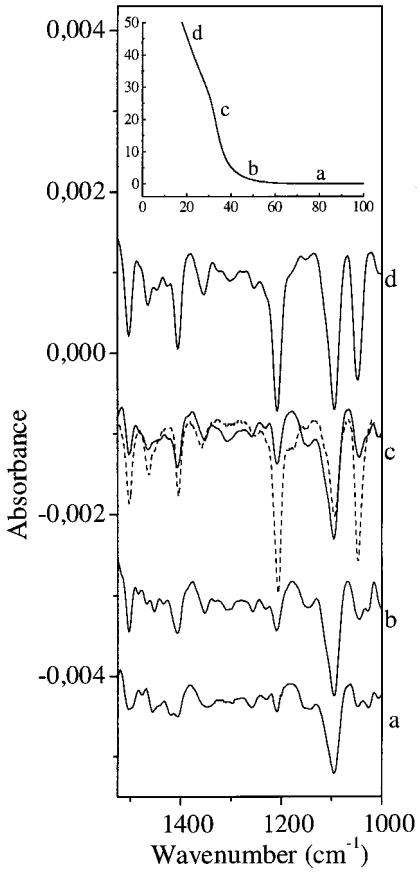

Figure 3. Reflection−absorption IR spectra of prec-DMePPV at the air−water interface. Experimental spectra (solid lines) of prec-DMePPV, area per repeating unit: 80 Å² (a), 52 Å² (b), 35 Å² (c), and 25 (d) Å². Calculated spectrum ((c) dashed line) of a nonoriented film of prec-DMePPV of 8.7 Å thickness (details in the Experimental Section). $T = 20$ °C. The spectra were *Y*-shifted without stretching out the spectra.

3c, solid line) the spectrum has to be compared with the calculated spectrum of Figure 3c (dashed line). This calculated spectrum can be seen as a reflection spectrum of a nonoriented, 8.7 Å thick prec-DMePPV film at the air−water interface measured with the same optical setup. This thickness corresponds with the thickness of a monolayer with an area 35 Å² per repeating unit. The thickness was calculated assuming that the density of the monolayer is 1.1 g/cm³.

Comparing the solid line and dashed line in Figure 3c, it can be seen that the intensities of the absorption bands at 1502 and 1407 cm^{-1} are much lower in the measured spectrum than the intensity of these bands in the calculated spectrum. These bands have been ascribed to semicircular phenyl stretches (Table 1). The transition moments of these bands are lying in the plane of the phenyl ring. The low intensity of these phenyl bands agrees with the fact that the rings are almost perpendicular to the water surface because should the ring phenyl lie flat at the air−water interface, the intensities of these bands would be much higher than the intensities of the calculated spectrum.

The intensity of the band of the methoxy-leaving group at 1096 cm^{-1} is almost equal in the measured and calculated spectrum. This means that either this band is not oriented or the transition moment makes an angle close to 54.7 ° with the air−water interface.[44]

The bands at 1204 and 1044 cm^{-1} can be attributed to aromatic ether stretch vibrations (Table 1). To establish the orientation of the aromatic ring, the direction of the transition dipole moment of the absorp-

Table 1. Assignments of IR Absorption Bands prec-DMePPV[47,48]

wavenumber(cm^{-1})	assignment	dipole transition moment
1502	semicircular phenyl stretch	in the plane of phenyl ring
1464	$\delta_{as}(CH_3)$ asym bending and $\delta(CH_2)$ scissors	
1407	semicircular phenyl stretch	in the plane of phenyl ring
1350	$\delta_s(CH_3)$ sym bending aliph and arom ether	
1204	ν(aryl oxygen) (arom methoxy group)	=C−O direction, in plane of phenyl ring
1096	ν_a(COC), aliph (methoxy leaving group)	|| to C−C direction
1044	ν(alkyl oxygen) (arom methoxy group)	O−C direction

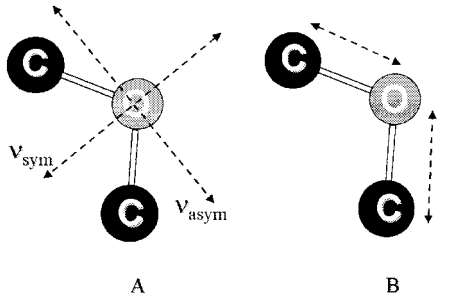

Figure 4. Transition dipole moment directions of the ether vibrations: (A) the ether vibrations are coupled and (B) the ether vibrations are not coupled.

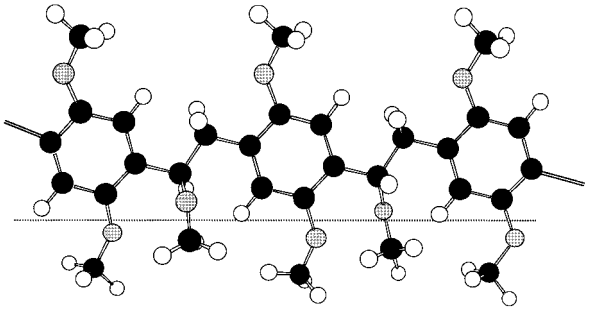

Figure 5. Side view of the orientation of prec-DMePPV at the air−water interface: carbon, black atoms; oxygen, gray atoms; hydrogen, white atoms.

tion must be known. Some authors suppose that these vibrations are coupled, resulting in a symmetric and an asymmetric C−O−C mode.[45,46] When the vibrations are coupled, the transition dipole moment directions of the symmetric and asymmetric mode are perpendicular, as shown in Figure 4A.

However, others suppose that coupling of these modes is not strong because the aromatic ring is considerably different from a methyl group.[47,48] In this case, the mode at 1204 cm^{-1} is principally the aromatic carbon−oxygen stretch frequency and the mode at 1044 cm^{-1} is the aliphatic carbon−oxygen stretching frequency. The transition moments of these carbon−oxygen stretch frequencies are mainly directed along the carbon−oxygen bonds, as shown in Figure 4B. Liang et al. calculated on the basis of normal polarized transmission spectra of highly oriented, uniaxially drawn films of poly(*p*-2-methoxyphenylenevinylene) the angle of the transition dipole moments of the aromatic ether groups with the chain axis.[49] From these results it can be calculated that the angle between the transition moments of the ether vibrations is 23°. Should the ether vibrations be coupled, the angle between the transition dipole moments would be independent of the bond angle of the aromatic ether and would be equal to 90°. So, it can be concluded that the vibrations of such aromatic ether groups are not strongly coupled and that the transition dipole moment direction is lying along the carbon−oxygen bonds (Figure 4B). When the solid line is compared with the dashed line of Figure 3c, it can be seen that the intensities of both aromatic-ether bands are very low compared to the intensities of these peaks in the calculated spectrum. This means that both carbon−oxygen bonds of the aromatic-ether group are oriented perpendicularly to the water surface.

To gain a better insight into how the ether groups are oriented and the magnitude of the angles of the ether groups, we used an energy minimization program. As input for this program a model monolayer of prec-DMePPV was built up. The building block used for this model was an oligomer consisting of five repeating units of prec-DMePPV. The aromatic rings of the oligomer were oriented perpendicularly to the imaginary water surface to imitate the situation of a prec-DMePPV monolayer at the air−water. Five of these oligomers were closely packed in such a way that the area per repeating unit was about 38 $Å^2$/repeating unit. Subsequently, the energy of the ether groups of the oligomers was minimized on the basis of the MM2 force field. After energy minimization the depicted structure of the oligomer in Figure 5 was obtained (only 2.5 repeating units are shown).

In Figure 5 the aromatic carbon−oxygen bond and the aliphatic carbon−oxygen bond of the aromatic-ether group are both to a large extent oriented perpendicularly to the air−water interface, which is in agreement with the low intensities of these bonds.

At 25 $Å^2$/repeating unit (Figure 3d) the collapse has already taken place, and the film has lost most of the orientation; therefore, the spectrum of Figure 3d resembles more or less the spectrum of a nonoriented film (Figure 3c, dashed line).

FT-IR reflection spectroscopy at the air−water interface was also done with prec-MEHPPV and prec-MePPV. On the basis of the absorption intensities of the aromatic-ether groups, it was also found that the aromatic rings are, even at large areas per repeating unit, more or less perpendicular to the water surface. This is in agreement with the assumptions made on the basis of the isotherms.

FT-IR reflection spectroscopy experiments at the air−water interface of prec-DBuPPV are shown in Figure 6.

The experimental spectra were taken at about 96 (a), 73 (b), 50 (c), 32 (d), and 21 $Å^2$/repeating unit (e); the corresponding positions in the isotherm are shown in the inset of Figure 6. It is only possible to take FT-IR spectra after the first transition, because at areas larger than 100 $Å^2$/repeating unit the intensity is too low compared to the noise.

The calculated reflection spectrum of an 11 Å thick prec-DBuPPV film at the air−water interface measured with the same optical setup is shown in Figure 6d (dashed line). The thickness of this calculated spectrum corresponds to a monolayer with 32 $Å^2$/repeating unit assuming a density of 1.1 g/cm^3. The assignments of the

Table 2. Assignments of IR Absorption Bands prec-DBuPPV[47,48]

wavenumber (cm^{-1})	assignment	dipole transition moment
1502	semicircular phenyl stretch	in the plane of the phenyl ring
1471	$\delta(CH_2)$ scissors	
1413	semicircular phenyl stretch	in the plane of the phenyl ring
1380	$\delta_s(CH_3)$ sym bending	
1357	$\delta_s(CH_3)$ sym bending of the aliph ether	
1201	ν(aryl oxygen) (arom butoxy group)	=C−O direction, in plane of the phenyl ring
1096	ν_a(COC), aliph (methoxy leaving group)	|| to C−C direction
1033	ν(alkyl oxygen) (arom butoxy group)	O−C direction

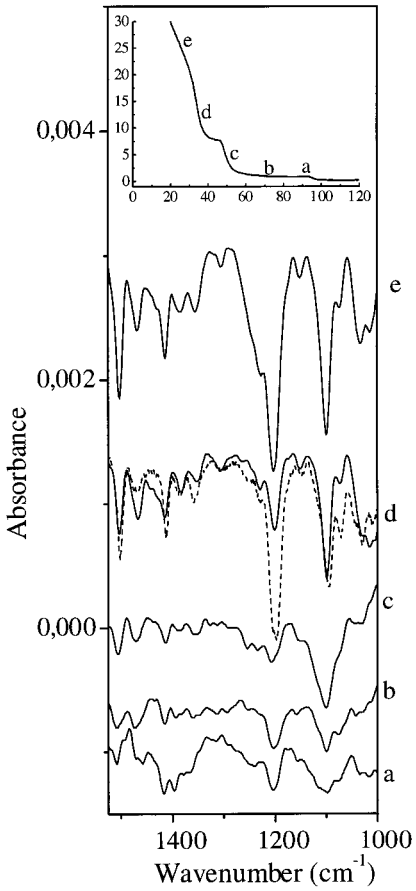

Figure 6. Reflection−absorption IR spectra of prec-DBuPPV at the air−water interface. Experimental spectra (solid lines) of prec-DBuPPV, area per repeating unit: 96 Å^2 (a), 73 Å^2 (b), 50 Å^2 (c), 32 (d) Å^2, and 25 Å^2 (e). Calculated spectrum ((d) dashed line) of a nonoriented film of prec-DBuPPV of 11 Å thickness (details in the Experimental Section). T = 15 °C. The spectra were Y-shifted without stretching out the spectra.

transition moments and the transition dipole moment directions of the bands of prec-DBuPPV are given in Table 2.

In the spectra of the monolayers with 96 Å^2/repeating unit and 73 Å^2/repeating unit (Figure 6, a and b) the band at 1201 cm^{-1} is fairly strong compared to the rest of the peaks, and at 50 and 32 Å^2/repeating unit (Figure 6, c and d) the intensity of this peak is relatively weak. The transition dipole moment of this peak is lying in the direction of the aromatic carbon−oxygen bond and therefore directed in the plane of the ring. So, it can be concluded that, in contrast to what was found for prec-DMePPV, the aromatic ring of prec-DBuPPV takes on a more planar orientation at large areas per repeating unit. However, at areas smaller than about 50 Å^2/repeating unit the aromatic ring takes on, just as prec-DMePPV, an almost fully perpendicular orientation with respect to the water surface. This in agreement with the assumptions made from the surface-pressure

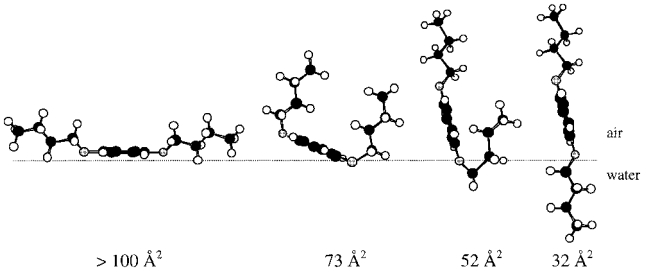

Figure 7. Side view of the conformations of the aromatic ring of prec-BuMePPV. Area per repeating unit: >100, 73, 52, and 32 Å^2. Carbon, black atoms; oxygen, gray atoms; hydrogen, white atoms.

isotherms that the repeating unit of prec-DBuPPV is lying completely flat on the water surface at areas >100 Å^2/repeating unit. This conformation is shown in Figure 7, >100 Å^2. (For clarity, only the aromatic ring of the repeating unit and not the aliphatic part is drawn in Figure 7.)

The aromatic rings of precursors that are asymmetrically substituted with alkyl chains or that are not substituted with alkyl chains take on, directly after spreading, a perpendicular orientation with strong lateral cohesive forces between the backbone elements. The alkyl chains of the asymmetrically substituted precursors are directed out of the water subphase. The most prominent cohesive interactions are $\pi-\pi$ interactions between the aromatic rings. Prec-DBuPPV is symmetrically substituted, and therefore such a perpendicular orientation of the aromatic ring is hindered because in this orientation one of the hydrophobic alkyl chains per repeating unit is forced into the water subphase. The copolymer consists for 50% out of prec-DBuPPV units and is also symmetrically substituted but shows no transitions. Apparently, in the copolymer case, the repulsive interactions of the alkyl chains by water subphase are overruled by the favorable cohesive interaction between the aromatic rings. Prec-DBuPPV is assumed to be in an expanded state at large areas per repeating unit because in the parallel orientation of the aromatic rings all the ether groups are in contact with the water subphase, which brings about large adhesive interactions with water. Moreover, in this orientation no large cohesive interactions are possible between the aromatic rings, and strong cohesive interactions between the rather short butyl chains are very unlikely. However, the surface pressure is zero at large areas per repeating unit. This is in contradiction with what is normally found for an expanded monolayer but can be explained by the fact that a prec-DBuPPV chain forms at large areas, as shown in Figure 8, a "rodlike" molecule, with low rotational motions.

We assume that these rods distribute homogeneously at the water surface and are pushed together at the first transition. It is assumed that upon further compression, as can be seen in Figure 7, the butyl groups are pushed

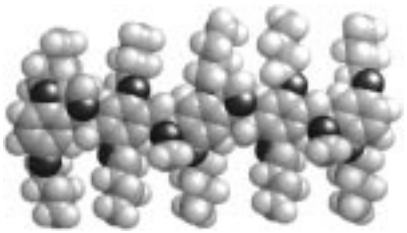

Figure 8. Water side view of a space-filling model of a rodlike prec-DBuPPV chain at large areas per repeating unit.

away from the water surface, and the aromatic ring takes on more and more a tilted conformation until an orientation drawn in Figure 7, 52 Å^2, is obtained. This orientation is enforced by the supplied pressure and is not very favorable because only two of the three ether groups of the repeating unit are in contact with the water subphase, and no interaction between the aromatic rings is possible. Subsequently, at the second transition one butyl chain per repeating unit is forced into the water layer, and favorable lateral face-to-face interactions between the aromatic rings are obtained (Figure 7, 32 Å^2).

Hysteresis Experiments. Hysteresis experiments can be carried out to elucidate whether processes that take place in the monolayer during compression are irreversible or not. It was assumed above that in the case of prec-DBuPPV there are no cohesive interactions between the chains until the second transition. The state that is obtained due to cohesive interactions is mostly irreversible, therefore, hysteresis experiments were used to confirm the assumptions we made concerning the monolayer behavior of the precursor polymers.

The hysteresis experiments of prec-DBuPPV and prec-DMePPV are shown in Figure 9, A and B, respectively. Hysteresis experiments of prec-DBuPPV performed with a maximum pressure of 7 mN/m, which is before the second transition in the isotherm, showed that no irreversible processes occurred (Figure 9A, lower curves), because the second cycle does not differ from the first. Hysteresis experiments with a maximum surface pressure of 15 mN/m, which is beyond the second transition in the isotherm, show that under the influence of the increased surface pressure irreversible processes in the monolayer have occurred (Figure 9A, upper curves). In Figure 9B it can be seen that compression of the prec-DMePPV up to 7 and 15 mN/m both result in the first cycle being different from the second cycle. So, in contrast to prec-DBuPPV, prec-DMePPV shows hysteresis in both cases. These results are in correspondence with the assumptions already made concerning the conformations of the monolayers of prec-DBuPPV and prec-DMePPV. Prec-DMePPV takes on directly after spreading a conformation with $\pi-\pi$ interactions between the aromatic rings. The hysteresis is very likely caused by increase of irreversible lateral interactions between the aromatic rings during compression. When prec-DBuPPV is compressed until 7 mN/m (before the second transition), the butyl chains are oriented out of the interface and prevent $\pi-\pi$ interactions between the aromatic rings, and no hysteresis is observed. However, after the second transition (compression to a maximum value of 15 mN/m) one butyl chain is pushed into the water phase, and the butyl chains can no longer prevent the $\pi-\pi$ interactions between the aromatic rings and hysteresis is observed.

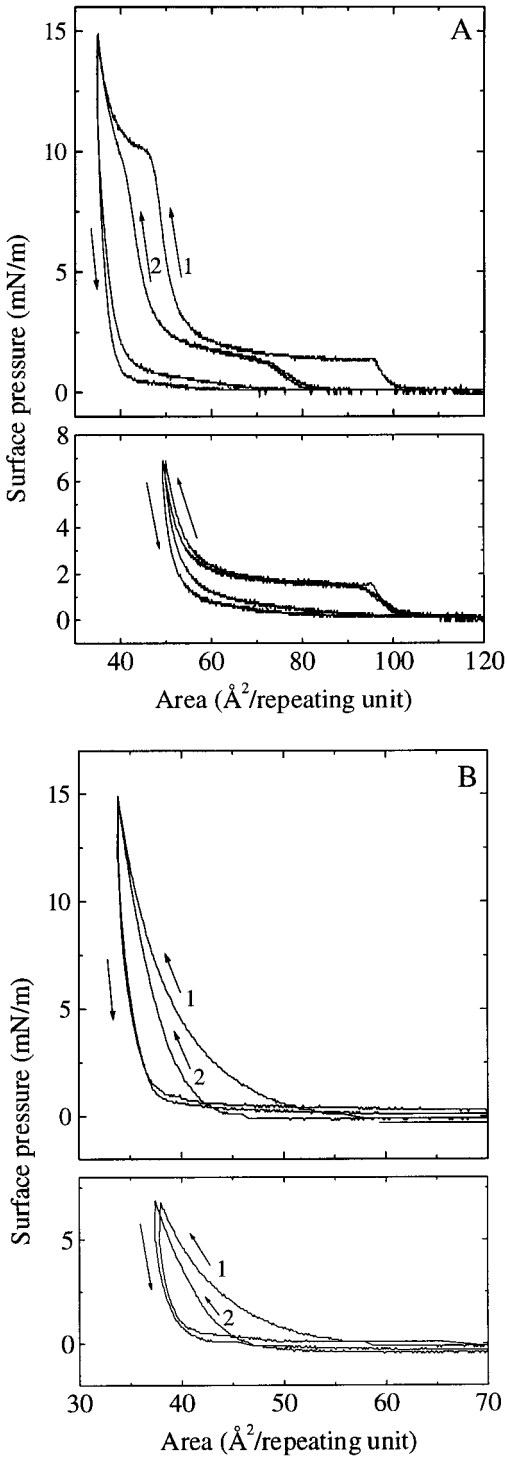

Figure 9. Hysteresis isotherms of (A) prec-DBuPPV and (B) prec-DMePPV. Upper curves: maximum pressure set at 15 mN/m. Lower curves: maximum pressure set at 7 mN/m, T = 10 °C, compression speed = 1 Å^2/(repeating unit min).

Conclusions

All the alkoxy-substituted precursor PPVs studied form real polymer monolayers at the air−water interface, and no surface pressure gradients are formed during compression. The surface pressure isotherms of prec-MePPV, prec-DMePPV, prec-BuMePPV, copolymer, and prec-MEHPPV show no special transitions; the closely packed monolayer is formed in the range of 36−45 Å^2/repeating unit, and the monolayers can be considered to be a 2-D "collapsed" state. Directly after

spreading the aromatic rings of these, polymers are oriented almost perpendicularly to the surface. The isotherm of prec-DBuPPV shows two transitions because the ring is, in contrast to the other precursors, (di)substituted with a longer alkyl chain. Therefore, the side chains dominate the configuration and orientation of the molecules. The prec-DBuPPV monolayer is assumed to be in the expanded state at large areas per repeating unit. Until the first transition the repeating units of prec-DBuPPV are lying flat at the air−water interface. During further compression the butyl chains are pushed out of the air−water interface, and the rings take on a more tilted orientation. At the second transition one butyl chain per repeating unit is pushed into the water phase, and the aromatic ring is oriented almost perpendicularly to the air−water interface.

References and Notes

(1) Gaines, G. L. *Insoluble Monolayers at Liquid−Gas Interfaces*; Interscience: New York, 1966.
(2) Ulman, U. *An Introduction to Ultrathin Organic Films: From Langmuir−Blodgett to Selfassembly*; Academic Press: Boston, 1991.
(3) Stenhagen, E. *Trans. Faraday Soc.* **1938**, *34*, 1328.
(4) Gaines, G. L.; Roberts, R. W. *Nature (London)* **1963**, *197*, 787.
(5) Nasilli, C.; Rabe, J. P.; Rabolt, J. F.; Swalen, J. D. *Thin Solid Films* **1985**, *134*, 173.
(6) Tieke, B.; Weiss, K. *J. Colloid Interface Sci.* **1984**, *101*, 129.
(7) Brenton, M. *J. Macromol. Sci., Rev. Macromol. Chem.* **1981**, *C21*, 61 and references therein.
(8) Tredgold, R. H.; Winter, C. S. *J. Phys. D: Appl. Phys.* **1982**, *15*, L55.
(9) Rubner, M. F. In *Polymers for Electronic and Photonic Applications*; Wong, C. P., Ed.; Academic Press: Boston, 1993; p 601.
(10) Swalen, J. D.; Allara, D. L.; Andrade, J. D.; Chandross, E. A.; Garoff, S.; Israelachvili, J.; McCarthy, T. J.; Murray, R.; Pease, R. F.; Rabolt, J. F.; Wynne, K. J.; Yu, H. *Langmuir* **1987**, *3*, 932.
(11) Rubner, M. F.; Scotheim, T. W. In *Conjugated Polymers:* Brédas, J. L., Silbey, R., Eds.; Kluwer Academic Publishers: Boston, 1991; p 363 and references therein.
(12) Decher, G.; Hong, J. D.; Schmitt, J. *Thin Solid Films* **1992**, *210/211*, 831.
(13) Miyashita, T. *Prog. Polym. Sci.* **1993**, *18*, 263.
(14) Fox, H. W.; Tayler, P. W.; Zisman W. A. *Ind. Eng. Chem.* **1947**, *39*, 1401.
(15) Adam, N. K.; Harding, J. B. *Proc. R. Soc. London* **1934**, *A134*, 104.
(16) Alexander, A. E. *Trans Faraday Soc.* **1941,** *37*, 426.
(17) Beredjick, N.; Rives Jr., H. E. *J. Polym. Sci.* **1962**, *62*, S64.
(18) Isemura, T.; Hotta, H.; Miwa, T. *Bull. Chem. Soc. Jpn.* **1953**, *26*, 380.
(19) Malcolm, B. R. *Proc. R. Soc. London* **1968**, *A305*, 363.
(20) Orthmann, E.; Wegner, G. *Angew. Chem., Int. Ed. Engl.* **1986**, *25*, 1105.
(21) Schoondorp, M. A.; Vorenkamp, E. J.; Schouten, A. J. *Thin Solid Films* **1991**, *196*, 121.
(22) Teerenstra, M. N.; Vorenkamp, E. J.; Schouten, A. J. *Thin Solid Films* **1991**, *196*, 153.
(23) Brinkhuis, R. H. G.; Schouten, A. J. *Macromolecules* **1992**, *25*, 2717.
(24) Marks, R. N.; Halls, J. J. M.; Bradley, D. D. C.; Friend, R. H.; Holmes, A. B. *J. Phys.: Condens. Matter* **1994**, *6*, 1379.
(25) Rubner, M. F.; Skotheim, T. A. In *Conjugated Polymers*; Brédas, J. L., Silbey, R., Eds.; Kluwer: Dordrecht, 1991; p 363.
(26) Askari, S. H.; Rughooputh, S. D.; Wudl, F. *Synth. Met.* **1989**, *29*, 129.
(27) Lenz, R.; Han, C.; Stenger-Smith, J.; Karasz, F. *J. Polym. Sci., Part A: Polym. Chem. Ed.* **1988,** *26*, 3241.
(28) Tokito, S.; Momii, T.; Murata, H.; Tsutsui, T.; Saito, S. *Polymer* **1990**, *31*, 1137.
(29) Nishikata, Y.; Kakimoto, M.; Imai, Y. *Thin Solid Films* **1989**, *179*, 191.
(30) Wu, A.; Yokoyama, S.; Watanabe, S.; Kakimoto, M.; Imai, Y.; Araki, T.; Iriyama, K. *Thin Solid Films* **1994**, *244*, 750.
(31) Era, M.; Kamiyama, K.; Yoshiura, K.; Momii, T.; Murata, H.; Tokito, S.; Tsutsui, T.; Saito, S. *Thin Solid Films* **1989,** *179*, 1.
(32) Kim, J. H.; Kim, Y. K.; Sohn, B. C.; Kang, D.; Jin, J.; Kim, C.; Pyun, C. *Synth. Met.* **1995**, *71*, 2023.
(33) Shim, H. K.; Hwang, D. H. *Makromol. Chem.* **1993**, *194*, 1115.
(34) Delmotte, A.; Biesemans, M.; Rahier, H.; Gielen, M.; Meijer, E. W. *Synth. Met.* **1993**, *58*, 325.
(35) Mielczarski, J. A. *J. Phys. Chem.* **1993**, *97*, 2649.
(36) Brinkhuis, R. H. G.; Schouten, A. J. *Macromolecules* **1991**, *24*, 1496.
(37) Boven, G.; Brinkhuis, R. H. G.; Vorenkamp, E. J.; Schouten, A. J. *Macromolecules* **1991**, *24*, 967.
(38) *The Infrared Handbook*; Wolfe, W. L., Zissis, G. J., Eds.; IRIA: Office of Naval Research Institute of Michigan: Washington, DC; pp 4−43.
(39) *Molecular Mechanics*; Burkert, U., Allinger N. L., Eds.; American Chemical Society: Washington, DC, 1982.
(40) Crisp, D. J. In *Surface Phenomena in Chemistry and Biology*; Danielli, J. F., Pankhurst, K. G. A., Riddiford, A. C., Eds.; Perganon Press: New York, 1958; p 25.
(41) Malcolm, B. R. *Langmuir* **1995**, *11*, 204−210.
(42) Lemaire, B.; Bothorel, P. *Macromolecules* **1980**, *13*, 311.
(43) Kuzmenka, D. J.; Granick, S. *Macromolecules* **1988**, *21*, 779.
(44) Arndt, T.; Schouten, A. J.; Schmidt, G. F.; Wegner, G. *Makromol. Chem.* **1991,** *192*, 2215.
(45) *Principles and Practices of Infrared Spectroscopy*; Osland, R. C. J., Ed.; Pye Unicam Ltd.: Cambridge, 1985; p 29.
(46) *Infrared Characteristic Group Frequencies*; Socrates, G., Ed.; John Wiley & Sons Ltd.: New York, 1980; p 50.
(47) Katritzky, A. R.; Coats, N. A. *J. Chem. Soc.* **1959**, 2062.
(48) *Introduction to Infrared and Raman Spectroscopy*; Colthup, N. B., Daly, L. H., Wiberley, S. E., Eds.; Academic Press: New York, 1964.
(49) Liang, W.; Karasz, E. *Polymer* **1991**, *32*, 2363.

MA9900683